Optics Communications 451 (2019) 55–61

Contents lists available at ScienceDirect

Optics Communications

journal homepage: www.elsevier.com/locate/optcom

Low-cost multi-mode diode pumped Tm:YLF laser: Multi-color & Q-switching operations

Ersen Beyatli

Department of Electrical-Electronics Engineering, Recep Tayyip Erdogan University, Rize, 53100, Turkey

ARTICLE INFO

Keywords:
Lasers
Diode-pumped lasers
Tunable lasers
Infrared and far-infrared lasers
Multi-color lasers
Q-switched lasers

ABSTRACT

In this paper, we report a low-cost multi-mode AlGaAs laser diode pumped broadly-tunable solid-state Tm:YLF laser at room-temperature operating in two different regimes: multi-color and Q-switching. A low-cost multi-mode AlGaAs laser diode, driving 3 W power at 780 nm, was used to excite the 3% Tm^{3+}-ion doped YLF laser. In the continuous-wave regime, 650 mW of output power was obtained at 1942 nm with 41% power efficiency (indicates high cross-relaxation). The output wavelength can be tuned between 1831 and 2031 nm with a birefringent filter (BRF). To the best of our knowledge, this range is the broadest tuning range obtained from a Tm:YLF laser in 2 μm band. Furthermore, multi-color laser operations were observed by translating the crystal inside the cavity (without BRF) i.e. three two-color, two three-color and one four-color were obtained. As far as we know, these results are the first demonstration of three- and four-color 2 μm laser. Additionally, Q-switching regime were obtained by adding a saturable absorber into the cavity. In this regime, the repetition frequencies can be arranged between 16 and 100 kHz with a maximum of 2.7 W peak power and 2.39 μJ pulse energy by translating the saturable absorber along the stability region.

1. Introduction

Tm^{3+} doped solid-state laser systems are attracting a great deal of interest in the medical applications, remote sensing, atmospheric communication, spectroscopy and pumping of other laser systems [1]. These systems can lase at 2 μm (1.8–2.2 μm) region when they are pumped at 780 nm (±15 nm depending on the host crystal) band. To date, these Tm^{3+} laser systems have been pumped with a flash lamp [2,3], the output of Ti:Sapphire lasers [4,5] and AlGaAs diodes [6, 7]. Those systems are generally costly, bulky, inefficient and usually requires cooling mechanism. The best alternative method is using a low-cost commercially available AlGaAs laser diodes (designed for CD-Roms and laser printers) as a pump source. If these diodes are employed with a well-designed laser resonator, the Tm^{3+} doped laser systems could provide highly efficient 2 μm laser operations. So far, this idea has only been applied to the Tm:YAG laser system [8]. In that study, as high as 32 mW output power reported in continuous-wave regime. For the aforementioned areas, higher output powers and other regimes are needed for efficient integration.

Multi-color and Q-switching are two well-known operating regimes in the solid-state laser systems. Multi-color solid-state lasers are the result of more than one simultaneous wavelength oscillation in the laser resonator. This operation regime might bring great advantages to applications requiring more than one wavelength, such as biomedicine [9–11], coherent THz radiation [12,13], optical communications [14,15], laser ranging [16], remote sensing [17] etc. One technique for multi-color generation is using a gain medium which has multi-emission peaks. If the emission and gain cross-sections of these peaks are similar, there is a high probability that multi-color operation will be observed. Up to date, this technique has been used in many systems especially in Cr^{3+} [18–20], Nd^{3+} [21–23], Yb^{3+} [24] doped lasers. Similarly, in Tm^{3+} doped solid-state laser systems, there are only a few multi-color studies and mainly they have only two simultaneous oscillations [25–30].

Tm^{3+} doped YLF crystal also has many emission peaks [31]. As a result; to date; Tm:YLF lasers have been demonstrated at many different wavelengths e.g. 1885, 1902, 1909, 1940 nm [31–33]. However; to the best of our knowledge, a simultaneous operation of these wavelengths i.e. multi-color operation has only been obtained in [29]. In that study, the multi-color regime was achieved after introducing an extra birefringent element into the system, which reduced the compactness of the system. Also, in that study, only two-color results are reported.

In the Q-switching regimes, the output power is modulated with intracavity losses that results in nano-micro-second repetitive pulses. This regime is mainly used in industrial applications for laser cutting and welding, as well as in medical applications such as microsurgery [34]. In the Q-switching regimes, large upper state energy storage is essential, and one of the key point is the longer upper-state lifetimes (longer lifetime allows larger energy storage). In the Tm^{3+} doped crystals, fluoride hosts have longer upper-state lifetimes; and therefore, have great potential to operate in the Q-switching regime [35,36]. Currently, among the

E-mail address: ersen.beyatli@erdogan.edu.tr.

https://doi.org/10.1016/j.optcom.2019.06.027
Received 17 April 2019; Received in revised form 27 May 2019; Accepted 11 June 2019
Available online 19 June 2019
0030-4018/

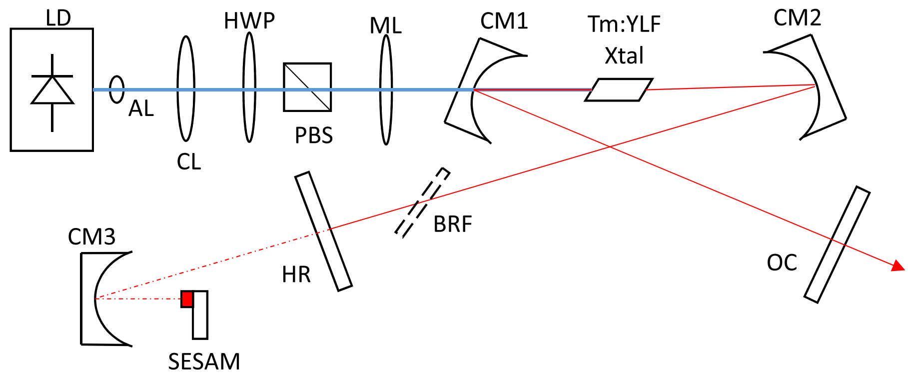

Fig. 1. A low-cost commercial multi-mode diode pumped multi-color & Q-switched Tm:YLF laser setup. LD: low-cost commercial multi-mode laser diode; AL: f = 4.51 mm Aspheric Lens; CL: f = 5 cm cylindrical lens; HWP: Half-wave plate; PBS: Polarizing Beam Splitter; ML: Spherical Lens with f = 5 cm; CM1: Curved Mirror with f = 5 cm; CM2: Curved Mirror with f = 7.5 cm; BRF: Birefringent Filter; HR: Highly Reflecting Mirror; CM3: Curved Mirror f = 1.9 cm; SESAM: Saturable Absorber; OC: Output Coupler.

Tm^{3+} doped fluoride crystals (i.e. YLF, LLF and BYF hosts) Q-switching regimes have been obtained with high peak powers and pulse energies but with relatively low frequencies (in the order of 100 Hz) [32,37–39]. Furthermore, in those studies, the repetition frequency was arranged by changing the input powers that directly affected the average output powers. For some applications, kHz level frequencies and the ability to directly control over the frequency (i.e. without changing the input power) could bring great advantages especially in medical applications.

In this study, we demonstrated a low-cost commercial AlGaAs laser diode (<250$) pumped Tm:YLF laser operating in two different regimes: multi- (two-, three- and four-) color and selective frequency Q-switching. By using a low-cost commercial laser diode with an optimized resonator, an output power up to 650 mW was attained with 41% power efficiency at 1942 nm. Higher than 40% power efficiency indicates high cross-relaxation effects in the system. Furthermore, the laser wavelength was tuned between 1831 and 2031 nm with a birefringent filter. To the best of our knowledge, this 200 nm tuning range is the broadest tuning range that is obtained from a quasi-3-level Tm:YLF solid-state laser systems to date. Moreover, when the Tm:YLF crystal translated along the stability region, multi-color (three two-color, two three-color and one four-color laser) operations were obtained at discrete locations of the crystal (without using the birefringent filter). As far as we know, these results are the first demonstration of multi-color (especially in the three-color and four-color cases) laser operations in the 2 μm regime. Also in this study, kHz level Q-switching regime was attained when a saturable absorber added into the resonator. The pulse repetition frequency was adjusted by simply translating the saturable absorber along the stability region, unlike the previous Tm^{3+} systems (i.e. not changing the input power). In this configuration, a repetition frequency ranging from 16 kHz to 100 kHz was attained in the Q-switching regime with a maximum of 2.7 W peak power and 2.39 μJ pulse energy. As far as we know, the repetition frequency arrangement in a Q-switched Tm:YLF laser (without changing the input power) is presented in this study for the first time. As a result, in this study, we have shown, for the first time, a low-cost diode pumped broadly tunable Tm:YLF laser operating in two different regimes: multi-color (i.e. two-, three- and four-color) and selective frequency Q-switching.

In the next section, the experimental setup will be explained in detail. Also, in the following section the continuous wave regime, multi-color regime and the selective frequency Q-switched results will be provided and discussed in detail.

2. Experimental setup

Fig. 1 shows the schematic of the diode-pumped Tm:YLF laser cavity. A low-cost commercial (<250 $) linearly polarized 3 W single-emitter multi-mode AlGaAs laser diode (LD) (from RPMC LDX-3315-780) was used for pumping at a central wavelength of 780 nm. These diodes are used in CD-roms and laser printers, and were therefore widely available. The LD had a transverse area 1 × 150 μm. The pump beam was diffraction-limited along the fast-axis (perpendicular to plane of junction) and multi-mode along the slow-axis. The pump beam was first collected with an aspheric lens (AL) with a focal length of f = 4.5 mm and then was collimated with a cylindrical lens (CL) with a focal length of f = 5 cm along the fast-axis. The input power was adjusted with a half-wave plate and (HWP) and a polarizing beam splitter cube (PBS). The pump beam was focused inside the laser crystal using a 5 cm focal length lens (ML), after passing through the PBS.

An astigmatically compensated 4-mirror X-cavity was used in the continuous-wave laser experiments. The X-cavity consisted of two curved mirrors (CM1 with f = 50 mm and CM2 with f = 75 mm), a highly reflecting mirrors (HR) and a wedged output coupler (OC). The cavity mirrors (CM1, CM2 and HR) had a reflectivity bandwidth from 1850 nm to 2200 nm, flat negative dispersion i.e. $-75\ fs^2$ between 1900 nm to 2100 nm and a transmission of ∼90% at the 780 nm. Short (OC) and long (HR) arm lengths were set to 11.5 cm and 28.5 cm, respectively. A 3% Tm^{3+} ion doped Brewster–Brewster c-cut (extraordinary axis is along the direction of propagation) 5-mm long YLF crystal was placed at Brewster angle inside the cavity. The crystal absorbed 73% of the 780 nm pump light under the lasing condition (under the non-lasing condition this value reduced to 65% due to pump saturation effects). Due to reflection losses of the pump optics and crystal transmission, maximum 1775 mW of the pump power was absorbed by the crystal under the lasing condition. According to ABCD analysis, the laser beam was focused inside the crystal with a spot size of 42 μm. Three different output couplers with 1.3%, 2.7% and 4.8% transmission percentages were employed in the continuous-wave experiments. A 3-mm-thick crystal quartz birefringent filter (BRF) with an optical axis 45° to the surface of the plate [40] was inserted into the cavity to tune the laser wavelength. It is important to note that; the system was operated at room temperature without using any cooling mechanism unlike any other Tm^{3+} doped laser systems.

In the BRF'less system, when the crystal was translated along the stability region, a sudden change in the output wavelength was observed and moreover multi-color regimes were attained. The results of 1.3% case (which had the most number of multi-color results) were carefully investigated and recorded.

In the Q-switching experiments, first, the HR mirror was replaced with a curved mirror (CM3 with f = 19 mm). The arm length was set to 37 cm in this case. A saturable absorber (SESAM obtained from BATOP) was placed at the focus of the CM3. The absorbance, the modulation depth, the saturation fluence and relaxation time constant of the SESAM were 2%, 1.2%, 70 $\mu J/cm^2$ and 10 ps respectively. The SESAM was glued on a glided Cu-cylinder sink and AR-coated for 2 μm (1700–2100 nm). By translating the SESAM around the focusing region, different Q-switching regimes were observed and recorded with high speed InGaAs detector. In these experiments, the estimated spot size (i.e. light radius) inside the crystal was changed between 15–30 μm.

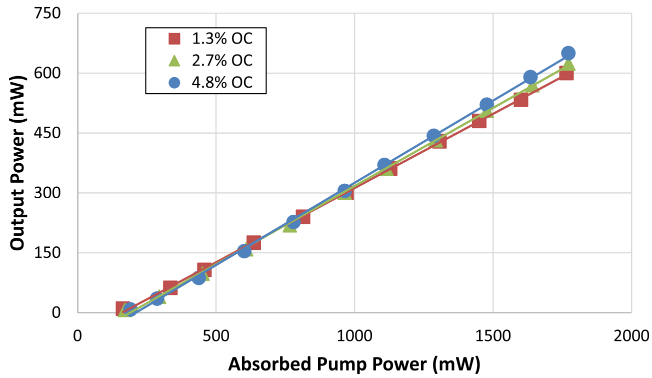

Fig. 2. Measured power efficiencies of the Tm:YLF laser pumped with a low-cost commercial multi-mode 3 W AlGaAs laser diode.

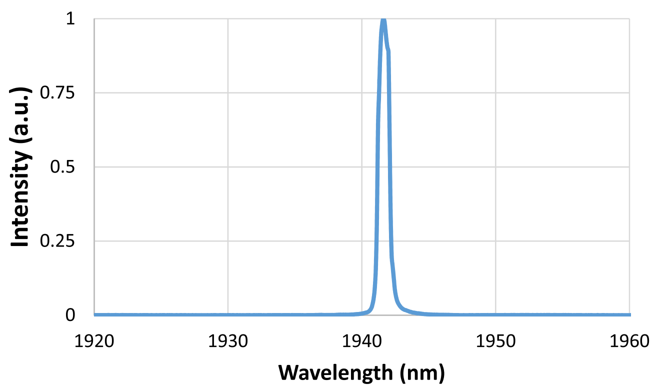

Fig. 3. Free running spectrum of the continuous-wave Tm:YLF laser obtained at highest output power of 650 mW.

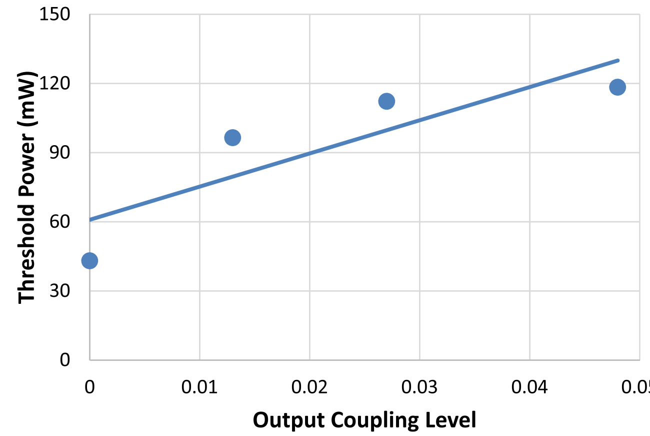

Fig. 4. Measured and best-fit variation of the absorbed threshold pump power as a function of the output coupler transmission for the Tm:YLF laser.

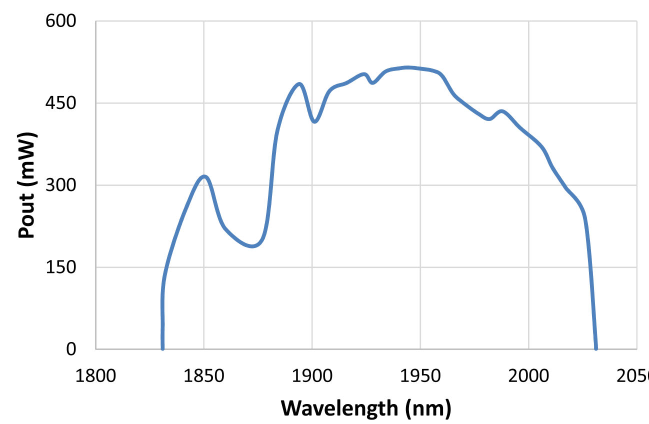

Fig. 5. Measured tuning curve of the Tm:YLF laser with 1.3% output coupling level. (A 3-mm quartz birefringent filter was used for tuning.)

3. Results and discussions

3.1. Continuous-wave results

Fig. 2 shows continuous-wave laser efficiencies taken with 1.3%, 2.7% and 4.8% output couplers. The best output power performance was attained with the 4.8% output coupler where 650 mW output power was obtained with a slope efficiency of more than 41% at 1942 nm (Fig. 3). In this output coupling level, the threshold absorbed pump power was 118 mW. According to Findlay–Clay analysis [41], having more than 40% (i.e. theoretical limit = 780 nm/1942 nm) slope efficiency implies high cross-relaxation effects in the laser system.

With 2.7% output coupler, the maximum attained output power was 624 mW. In this case, the slope efficiency became 39% and the lasing threshold was 112 mW. At the 1.3% output coupling level, these numbers became 600 mW for the maximum output power, 37% for the slope efficiency and 96 mW for the lasing threshold. In these results, we have observed that an increase in the output coupling level yields a higher slope efficiency and a higher threshold level; which are in accordance with the Caird theory [42].

Fig. 4 shows the measured variation of the absorbed threshold pump power as a function of the output coupler transmission. Here, the absorbed threshold pump power was also measured with a highly reflecting output coupler in addition to the output couplers. In the limit of vanishing output coupling, the absorbed threshold pump power reduced to as low as 43 mW. By assuming that the incident threshold pump power (P_{th}) varies linearly with the total cavity loss according to

$$P_{th} = C(T + L) \tag{1}$$

the round-trip cavity loss was estimated to be 4.2% [43]. In Eq. (1), T is the transmission of the output coupler, L is the round-trip loss of the crystal, and C is a proportionality constant.

The gain profile (tuning range) of the system is shown in Fig. 5. In this experiment, the BRF was used with the 1.3% output coupler, because the lower loss level yielded lower lasing threshold, and therefore, a broader tuning range. The maximum output power was slightly lower in this case (for example, at the peak wavelength of 1942 nm, the output power decreased from 600 mW to 577 mW), due to the insertion of the BRF that introduced some unwanted losses. At room temperature, the continuous-wave laser wavelength could be tuned from 1831 nm to 2031 nm. To the best of our knowledge, this 200 nm tuning range is the broadest tuning range in a quasi-3-level Tm:YLF solid-state laser system. It should be also noted here that tuning on the short wavelength side was limited by the reflectivity bandwidth of the cavity high reflectors whose reflection reduced dramatically below 1850 nm. In the tuning regime; a deep was observed around 1875 nm possibly due to highly water absorption at that wavelength. Previously, similar broader tuning regimes again reached other Tm^{3+} doped fluoride crystals such as LLF [44] BYF [45] GLF [7]. In this study we achieved such broader range with a well-known Tm:YLF crystal.

3.2. Multi-color results

In the BRF'less system, when the crystal was translated between the curved mirrors, sudden wavelength changes were observed. Additionally, multi-color regimes were obtained at discrete locations. The

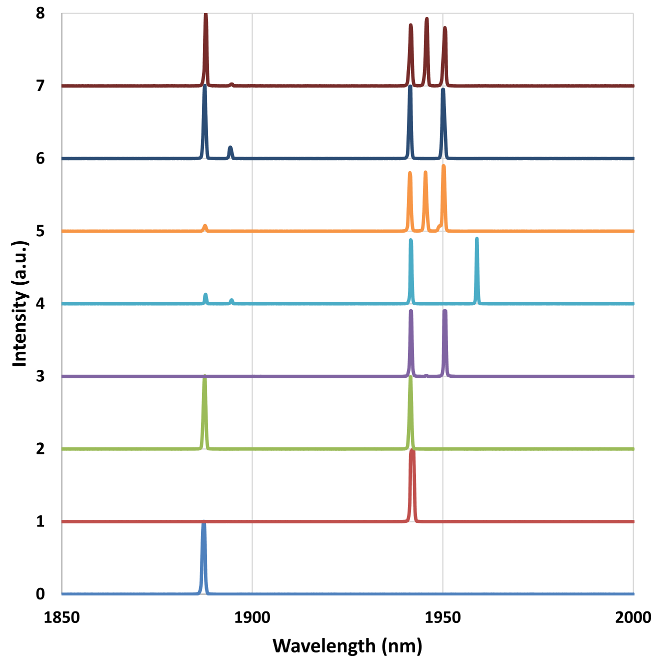

Fig. 6. Single-color and multi-color spectrums of the Tm:YLF laser without using the birefringent filter. The 0–1 and 1–2 intensity levels indicates the single color spectra; the 2–3, 3–4 and 4–5 intensity levels indicates two-color spectra; the 5–6 and 7–8 intensity levels indicates three-color spectra and the 7–8 intensity level indicates the four color spectra. (The results were recorded with the 1.3% output coupling level.)

spectrums (Fig. 6.) and results (tabulated at Table 1) were recorded for the 1.3% output coupler case. The free running spectrum (i.e. 1942 nm) is shown in Fig. 6's 1–2 intensity levels. While translating the Tm:YLF crystal, at some locations the output wavelength changed from 1942 nm to 1888 nm with lower output power i.e. 203 mW (Fig. 6's 0–1 intensity level). Along the stability region, three different dual-wavelength transition pairs were observed with different output powers. 1888 nm & 1942 nm and 1942 nm & 1959 nm wavelength pairs (Fig. 6's 2–3 and 4–5 intensity levels) had more than 250 mW output power, and the 1942 nm & 1951 nm wavelength pair had more than 500 mW output power (Fig. 6's 3–4 intensity level). An additional two different three-color and one four-color regimes were observed at some other locations. In the three-color case, the 1888 nm & 1942 nm & 1951 nm triplets had an almost 200 mW output power (Fig. 6's 6–7 intensity level) whereas 1942 nm & 1946 nm & 1951 nm triplets had more than a 300 mW output power (Fig. 6's 5–6 intensity level). In the four-color regime 1888 nm, 1942 nm, 1946 nm and 1951 nm simultaneous wavelength oscillations were observed in the cavity with an almost 400 mW output power (Fig. 6's 7–8 intensity level). These multi-color regimes are quite stable (more than 15 min) which was enough for the applications mentioned in the introduction. Also these regimes can be reproduced when the crystal is positioned at the same location. Furthermore, the multi-color regimes are input power dependent. For example, at the location of the four-color oscillation; four color regime can be obtained when the absorbed pump power was more than 1450 mW. At the same location, three-color oscillation was observed between 1450 to 1300 mW absorbed pump power. Two-color oscillation was observed between 750 to 1300 mW absorbed pump power. Less than 750 mW, only one wavelength oscillation was observed. The detailed power efficiency graph was shown in Fig. 7. Currently, two-color results have been observed and recorded in some other Tm^{3+} doped laser systems [25,27]. However, as far as we know, the three- and four-color regimes were not previously achieved in any Tm^{3+} doped laser system.

The output laser beam is π-polarized. Therefore, the beam is also π-polarized inside the cavity and propagates along the c-axis of the

Table 1
Multi-color Tm:YLF laser results.

Number of wavelengths	Wavelengths (nm)	Output power (mW)
1	1888	203
	1942	600
2	1888, 1942	284
	1942, 1951	535
	1942, 1959	273
3	1942, 1946, 1951	316
	1888, 1942, 1951	194
4	1888, 1942, 1946, 1951	396

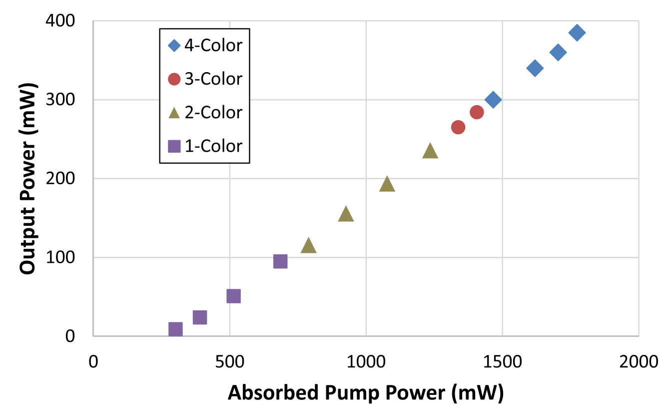

Fig. 7. Power efficiency curve of the 4-color laser operation. At different absorbed pump power level we have different number of wavelength oscillations. Up to 750 mW absorbed pump power, only one wavelength oscillation was observed. Between 750 to 1300 mW, two-color laser operation was observed. Between 1300 to 1450 mW, three-color laser operation was observed. Four-color laser operation was observed when the absorbed pump power was more than 1450 mW.

crystal. In the emission spectrum of the c-cut Tm:YLF crystal, two main peaks were observed in the π-polarized spectrum i.e. 1830 nm and 1880 nm [31] and their gain cross-sections are very high (Fig. 8). These wavelengths shift to longer wavelengths in the laser oscillations. In our case, the 1830 nm peak shifted to 1888 nm and the 1880 nm peak shifted to 1942 nm. Two-color operation was obtained at 1888 nm and 1942 nm (Fig. 6's 2–3 intensity level) with the simultaneous oscillation of these two peaks. Also, the emission spectrum band of 1880 nm (which shifts to 1942 nm) was relatively broader. This fact led to two- and three-color laser operations in the system (Fig. 6's 3–4, 4–5 and 5–6 intensity levels). Together with 1830 nm band (shifts to 1888 nm), we obtained three- and four-color laser operations (Fig. 6's 6–7 and 7–8 intensity level).

A closer look into the 1942 nm & 1951 nm wavelength pair spectrum; it can be observed a tendency of two more (i.e. 1888 nm and 1894 nm) wavelength oscillations. Similarly, in the three-color cases, an 1888 nm tendency was observed in the 1942 nm & 1946 nm & 1951 nm wavelength triplets and an 1894 nm tendency was observed in the 1888 nm & 1942 nm & 1951 nm wavelength triplets. In the four-color regime, an 1894 nm tendency was also observed as a fifth wavelength. A different doping level or length of crystal might result in these wavelengths' oscillations in the same resonator. Thus, a five-color laser operation at 2 μm region could also be possible. Furthermore, in the different doping level or length of the Tm:YLF crystal, there is also a highly possible scenario that any combination of these six individual wavelengths could be simultaneously oscillated in the laser resonator. (For example, with a different percentage Tm^{3+} doped or a longer/shorter Tm:YLF crystal, 1942 nm, 1946 nm, 1951 nm and 1959 nm wavelengths could oscillate simultaneously inside the system.)

3.3. Q-switching results

The Q-switching regime was obtained after adding the SESAM into the cavity. The output wavelength in this regime was 1888 nm (Fig. 9)

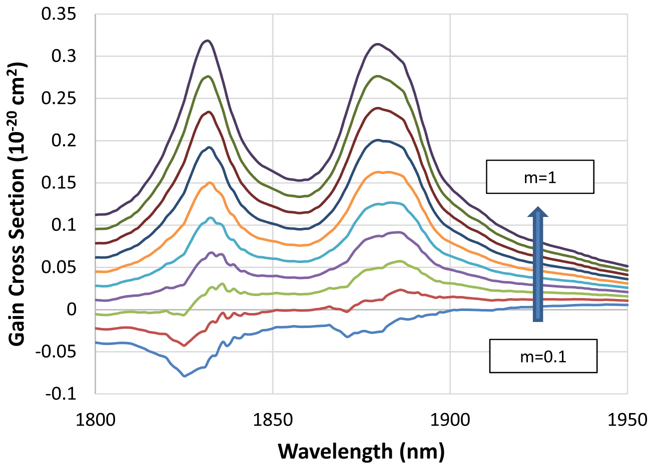

Fig. 8. Estimated Gain Curve of the Tm:YLF crystal (m is the inversion ratio).

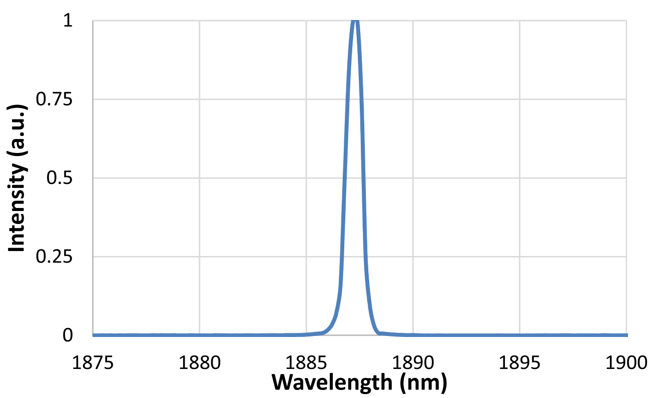

Fig. 9. Free-running spectrum of the Q-switched Tm:YLF laser.

as opposed to the cw regime (i.e. 1942 nm). When we look at the gain cross-section in detail, we observe that at high level of inversion ratio, the 1830 nm peak (shifts to 1888 nm) have slightly higher gain cross-section (Fig. 8). In the Q-switching regime, since the laser is on for a short period of time and is off rest of the period, the population inversion ratio ratio will increase a lot during the off-state (and could become close to 1). Hence, the shorter wavelength oscillation was observed in the Q-switching regime (as in [46,47]). And also one another possible reason is the 1880 nm peak (shifts to 1942 nm) have higher loss after insertion of an extra curved mirror and a SESAM into the cavity. That also affects the oscillated wavelength.

The repetition frequency can be adjusted by translating the SESAM along the stability region (i.e. all SESAM locations where stable laser operations were obtained without changing any other element locations). Some of the results are tabulated in Table 2. In those regimes the repetition frequency varied between 16 kHz (Fig. 10) and 100 kHz (Fig. 11). Up to 2.7 W peak power and 2.39 μJ pulse energy was obtained in this translating process. Unlike the previous Tm^{3+} doped fluoride laser systems [32,37–39,48], the frequency arrangement was done with the translation of the SESAM along the stability region. The pulse widths are around μs range, because the modulation depth is relatively low (i.e. 1.2%) compared to the previous Tm^{3+} based nanosecond Q-switched lasers (181 ns with 19.6% in [25], 7.6 ns with 22% in [39], 25 ns with 22% in [49]).

In the standard passive Q-switching theory, the repetition frequency can be estimated from [50,51]

$$f_{rep} = \frac{1}{\tau_f}\frac{G_0}{2Q_0} \tag{2}$$

Here, f_{rep} is the repetition frequency, τ_f is the fluorescence lifetime (15.6 ms for Tm:YLF crystal [52]), G_0 is the round-trip small-signal gain and Q_0 is the modulation depth of the absorber (in our case 1.2%). In this Eq. (2), τ_f and Q_0 are fixed and depend on the materials. Whereas G_0 depends on many factors including the pump beam and the laser beam mode-matching inside the crystal. The cavity length (yielding the effective cross-sectional area) and also the alignment of the laser beam inside the crystal were changed by translating the SESAM. These two factors directly affects the pump–laser beams mode-matching, thus, the G_0. As a result, changing the SESAM location yields an increase/decrease in the repetition frequency f_{rep}.

On the other hand, the output power can be estimated from

$$P_{out} = T\frac{P_{sat}}{2}\left(\frac{G_0}{G_{th}} - 1\right) \tag{3}$$

where T is the transmission percentage of the output coupler and G_{th} is the fractional threshold gain needed to reach lasing and can be expressed as $G_{th} = 1/2(L_c + T + Q_0)$ where L_c is the round-trip loss of the cavity [50,51]. In Eq. (3) P_{sat} is saturation power and can be calculated using

$$P_{sat} = \frac{h\vartheta_l}{\sigma_e \tau_f} A \tag{4}$$

where $h\vartheta_l$ is the laser photon energy, σ_e is the emission cross-section (3.7×10^{-21} cm^2 for Tm:YLF crystal [52]) and A is the effective cross-sectional area of the laser beam inside the Tm:YLF crystal.

As previously stated changing the SESAM location affects G_0, and thus the output power. A difference in the laser beam area inside the crystal directly affects the P_{sat} and thus the output power. As a result, the output power changes when we translated the SESAM along the stability region.

In the 16 kHz case, for example, the estimated area inside the crystal A was 2×10^{-3} mm^2 and therefore the saturated power P_{sat} became 34 mW. As a result, the estimated output power P_{out} was around 40 mW which was very close to the measured value of 38 mW. Similarly, for the 100 kHz case, the estimated area inside the crystal was 0.5×10^{-3} mm^2 and the saturated power P_{sat} became 8 mW. In this case the calculated output power is 63 mW which was again very close to the measured 62 mW of output power. Of course, the exact values depend on many other factors; however, these estimations are very close to the accurate results.

During the translation process, the mode-locking regime was not observed. The cavity mirrors had a flat dispersion in the 1900–2100 nm region and degrades outside this region. Since the output in the Q-switching region at 1888 nm, the second-order dispersion of the cavity was not compensated. To obtain mode-locking, one should use a cavity–mirror set with a different dispersive range. According to the tuning range (Fig. 5), there were two deeps around 1888 nm i.e. 1875 nm and 1901 nm. These deeps will most probably limit the spectral broadening in the mode-locking. So, using a flat dispersive mirror set covers 1875–1901 nm range will be a good choice to obtain mode-locking. Perhaps, in that case, adding extra dispersive elements such as YAG plates or CaF_2 prism pairs help to get mode-locking operation.

4. Conclusion

This study presented, a low-cost commercial multi-mode AlGaAs laser diode pumped broadly-tunable multi-color and Q-switched Tm:YLF laser at room-temperature. Using a low-cost commercially available laser diode, an output power of up to 650 mW was obtained at 1942 nm with 41% power efficiency. This power efficiency indicates highly cross-relaxation effect in the system. With a birefringent filter, the laser output could tune 200 nm in the 2 μm region, which is the broadest tuning range that has ever been reported from a Tm:YLF laser system. Moreover, different multi-color laser regimes were observed while translating the Tm:YLF crystal in the stability region. Three different two-color, two different three-color and one four-color laser

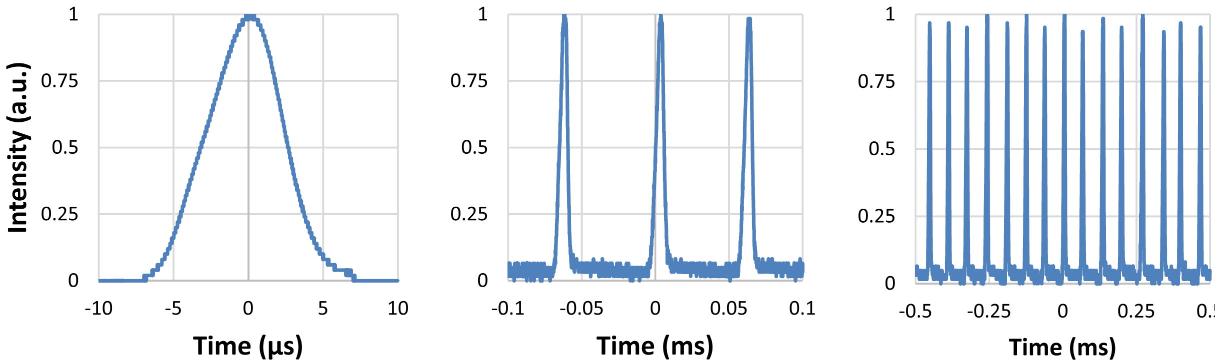

Fig. 10. 16 kHz repetition rate of the Q-switched Tm:YLF laser pulses in different time-scales. 38 mW average output power was obtained with 5.84 μs pulse widths, which corresponds to 0.41 W peak power and 2.39 μJ pulse energy.

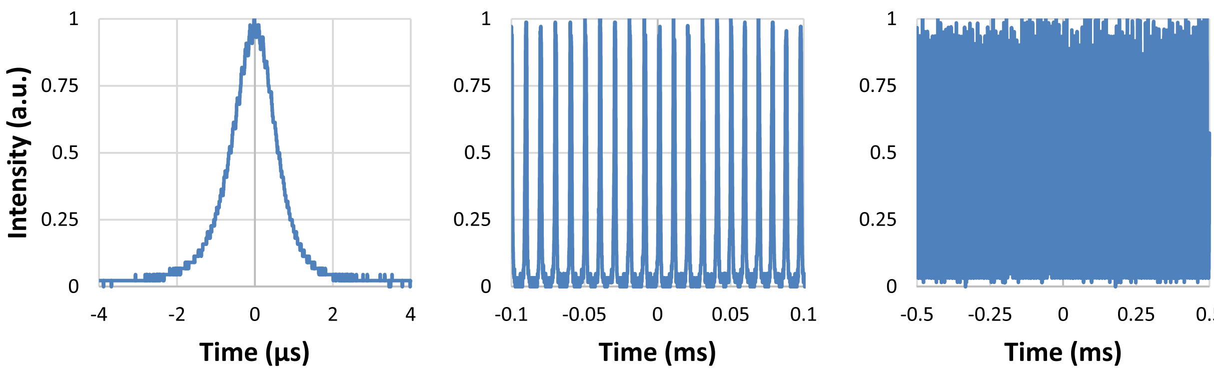

Fig. 11. 100 kHz repetition rate of the Q-switched Tm:YLF laser pulses in different time-scales. 62 mW average output power was obtained with 1.25 μs pulse widths, which corresponds to 0.5 W peak power and 0.62 μJ pulse energy.

Table 2
Q-switched Tm:YLF laser results.

Repetition frequency (kHz)	Output power (mW)	Pulse width (μs)	Peak power (W)	Pulse energy (μJ)
16	38	5.84	0.41	2.39
24	45	1.01	1.86	1.88
30	48	0.59	2.70	1.59
38	51	0.96	1.40	1.34
45	56	0.78	1.60	1.25
59	58	0.95	1.04	0.99
67	63	0.55	1.72	0.95
79	63	0.59	1.35	0.80
92	63	0.81	0.84	0.68
100	62	1.25	0.50	0.63

operations were obtained at some discrete locations. To the extent of our knowledge, these results are the first demonstration of three- and four-color laser oscillations in 2 μm region to date. These multi-color results have great potential to find applications in the biomedicine, optical communications and spectroscopy. Furthermore, the Q-switching regime was obtained by adding a SESAM into the cavity. In this regime, the repetition rates can be arranged between 16 kHz to 100 kHz by simply translating the SESAM along the stability region. Also, up to 2.7 W peak power and 2.39 μJ pulse energy was obtained while in translation. These Q-switching results also have potential to find applications in the industry and biomedical treatments.

Funding information

This work was supported in part by the Scientific and Technological Research Council of Turkey (TUBITAK) under grant 115F053.

References

[1] K. Scholle, S. Lamrini, P. Koopmann, P. Fuhrberg, 2 μm laser sources and their possible applications, in: S. Lamrini (Ed.), Frontiers in Guided Wave Optics and Optoelectronics, IntechOpen, Rijeka, 2010, Ch. 21.
[2] N.P. Barnes, K.E. Murray, M.G. Jani, R.L. Hutcheson, Flashlamp-pumped-room-temperature Ho:Tm:LuAG laser, 2379(1995) 2374–2379.
[3] T.-Y. Tsai, M. Birnbaum, Q-switched 2-μm lasers by use of a Cr^{2+}:ZnSe saturable absorber, Appl. Opt. 40 (36) (2001) 6633.
[4] R.C. Stoneman, L. Esterowitz, Efficient, broadly. tunable, Broadly tunable laser-pumped Tm:YAG and Tm:YSGG cw lasers, Opt. Lett. 15 (9) (1990) 486.
[5] X. Mateos, et al., Efficient 2-μm continuous-wave laser oscillation of Tm3+: KLu(WO4)2, IEEE J. Quantum Electron. 42 (10) (2006) 1008–1015.
[6] C. Bernardini, M. Tonelli, F. Cornacchia, D. Parisi, A. Toncelli, Efficient, diode-pumped Tm3+:BaY2F8 vibronic laser, Opt. Express 12 (9) (2004) 1982.
[7] A. Di Lieto, F. Cornacchia, N. Coluccelli, P. Laporta, G. Galzerano, M. Tonelli, High-efficiency diode-pumped Tm:$GdLiF_4$ laser at 19 μm, Opt. Lett. 34 (22) (2009) 3559.
[8] A. Wegrzyn, A. Rafalska-Łasocha, B. Dudek, R. Dziembaj, Nanostructured V-containing hydrotalcite-like materials obtained by non-stoichiometric anion exchange as precursors of catalysts for oxidative dehydrogenation of n-butane, Catal. Today 116 (1) (2006) 74–81.
[9] J. Wang, et al., Dual-wavelength laser speckle imaging to simultaneously access blood flow, blood volume, and oxygenation using a color CCD camera, Opt. Lett. 38 (18) (2013) 3690.
[10] C.W. Pirnstill, B.H. Malik, V.C. Gresham, G.L. Coté, In vivo glucose monitoring using dual-wavelength polarimetry to overcome corneal birefringence in the presence of motion, Diabetes Technol. Ther. 14 (9) (2012) 819–827.
[11] M.R. Jafarfard, S. Moon, B. Tayebi, D.Y. Kim, Dual-wavelength diffraction phase microscopy for simultaneous measurement of refractive index and thickness, Opt. Lett. 39 (10) (2014) 2908.
[12] K. Kawase, et al., Difference-frequency terahertz-wave generation from 4-dimethylamino-N-methyl-4-stilbazolium-tosylate by use of an electronically tuned Ti:sapphire laser, Opt. Lett. 24 (15) (1999) 1065.
[13] M. Scheller, J.M. Yarborough, J.V. Moloney, M. Fallahi, M. Koch, S.W. Koch, Room temperature continuous wave milliwatt terahertz source, Opt. Express 18 (26) (2010) 27112.
[14] S. Pan, X. Zhao, C. Lou, Switchable single-longitudinal-mode dual-wavelength erbium-doped fiber ring laser incorporating a semiconductor optical amplifier, Opt. Lett. 33 (8) (2008) 764.

[15] C.W. Chow, C.S. Wong, H.K. Tsang, All-optical NRZ to RZ format and wavelength converter by dual-wavelength injection locking, Opt. Commun. 209 (4–6) (2002) 329–334.
[16] J.B. Abshire, Pulsed multiwavelength laser ranging system for measuring atmospheric delay, Appl. Opt. 19 (20) (1980) 3436.
[17] R. Gaulton, F.M. Danson, F.A. Ramirez, O. Gunawan, The potential of dual-wavelength laser scanning for estimating vegetation moisture content, Remote Sens. Environ. 132 (2013) 32–39.
[18] D. Bruneau, H. Cazeneuve, C. Loth, J. Pelon, Double-pulse dual-wavelength alexandrite laser for atmospheric water vapor measurement, Appl. Opt. 30 (27) (1991) 3930.
[19] L. Kunpeng, et al., Dual-wavelength operation in all-solid-state Cr:LiSAF lasers with grating-controlled coupled-cavities, Opt. Laser Technol. 74 (2015) 1–5.
[20] H. Maestre, A.J. Torregrosa, J.A. Pereda, C.R. Fernández-Pousa, J. Capmany, Dual-wavelength Cr3+:LiCaAlF6solid-state laser with tunable THz frequency difference, IEEE J. Quantum Electron. 46 (11) (2010) 1681–1685.
[21] H.Y. Shen, et al., 10795- and 13414-nm: larger energy from a dual-wavelength Nd:$YAlO_3$ pulsed laser, Appl. Opt. 32 (30) (1993) 5952.
[22] J.L. He, et al., High efficiency single- and dual-wavelength Nd?: GdVO4lasers pumped by a fiber-coupled diode, 79 (3) (2004).
[23] T. Waritanant, A. Major, Dual-wavelength operation of a diode-pumped Nd:YVO4laser at the 1064.1 & 1073.1 nm and 1064.1 & 1085.3 nm wavelength pairs, Appl. Phys. B Lasers Opt. 124 (5) (2018) 87.
[24] R. Akbari, H. Zhao, A. Major, Dual-wavelength operation of a diode-pumped Yb:KGW laser, in: 2015 11th Conf. Lasers Electro-Optics Pacific Rim, CLEO-PR 2015, vo. 2, no. 7, 2016, pp. 1601–1604.
[25] H. Zhang, et al., Dual-wavelength, passively Q-switched Tm:YAP laser with black phosphorus saturable absorber, Opt. Mater. Express 6 (7) (2016) 2328.
[26] E.R. Hale, I. Divliansky, L. Glebov, Passively Q switched dual channel Tm:YLF laser by intracavity spectral beam combination with volume Bragg gratings, Opt. Express 26 (13) (2018) 16670.
[27] G. Li, B.Q. Yao, P.B. Meng, W. Wang, Y.L. Ju, Y.Z. Wang, InGaAs/GaAs saturable absorber for diode-pumped passively Q-switched mode-locking of Tm, Ho:YVO4laser, Laser Phys. Lett. 8 (1) (2011) 42–45.
[28] L.C. Kong, et al., Dual-wavelength synchronous operation of a mode-locked 2-μm Tm:$CaYAlO_4$ laser, Opt. Lett. 40 (3) (2015) 356.
[29] E. Beyatlı, U. Demırbas, Widely tunable dual-wavelength operation of Tm:YLF, Tm:LuAG, and Tm:YAG lasers using off-surface optic axis birefringent filters, Appl. Opt. 57 (23) (2018) 6679.
[30] I. Baylam, F. Canbaz, A. Sennaroglu, Dual-wavelength temporal dynamics of a gain-switched 2-μm Tm3+:Lu2O3 ceramic laser, IEEE J. Sel. Top. Quantum Electron. 24 (5) (2018) 1–8.
[31] A. Di Lieto, et al., Comparative spectroscopic and thermo-optic study of Tm:$LiLnF_4$ (Ln = Y, Gd, and Lu) crystals for highly-efficient microchip lasers at ∼2 μm, Opt. Mater. Express 7 (3) (2017) 844.
[32] Y. Dai, Y. Li, X. Zou, B. Jiang, Y. Hang, Y. Leng, Compact passively Q-switched tm:YLF laser with a polycrystalline cr:zns saturable absorber, Opt. Laser Technol. 57 (2014) 202–205.
[33] B.-Q. Yao, P.-B. Meng, G. Li, Y.-L. Ju, Y.-Z. Wang, Comparison of Tm:YLF and Tm:YAP in thermal analysis and laser performance, J. Opt. Soc. Amer. B 28 (8) (2011) 1866.
[34] D. Theisen-Kunde, V. Danicke, M. Wendt, R. Brinkmann, Temperature dependence of water absorption for wavelengths at 1920 nm and 1940 nm BT - 4th European Conference of the International Federation for Medical and Biological Engineering, 2009, pp. 2228–2229.
[35] F. Cornacchia, A. Di Lieto, M. Tonelli, LiGdF4:Tm3+: Spectroscopy and diode-pumped laser experiments, Appl. Phys. B Lasers Opt. 96 (2–3) (2009) 363–368.
[36] F. Cornacchia, A. Toncelli, M. Tonelli, 2-μm lasers with fluoride crystals: Research and development, Prog. Quantum Electron. 33 (2) (2009) 61–109.
[37] R. Faoro, et al., Passively Q-switched Tm:YLF laser, Opt. Lett. 37 (9) (2012) 1517.
[38] X. Mateos, et al., Passive Q-switching of a Tm:BaY2F8 laser, in: Cleo: 2013, 2013, p. CTu3D.8.
[39] H. Yu, V. Petrov, U. Griebner, D. Parisi, S. Veronesi, M. Tonelli, Compact passively Q-switched diode-pumped Tm:$LiLuF_4$ laser with 126 mJ output energy, Opt. Lett. 37 (13) (2012) 2544.
[40] U. Demırbas, Off-surface optic axis birefringent filters for smooth tuning of broadband lasers, Appl. Opt. 56 (28) (2017) 7815.
[41] D. Findlay, R.A. Clay, The measurement of internal losses in 4-level lasers, Phys. Lett. 20 (3) (1966) 277–278.
[42] J.A. Cairo, L.G. Deshazer, J. Nella, Characteristics of room-temperature 2.3-μm laser emission from Tm3+ in YAG and YAIO3, IEEE J. Quantum Electron. 11 (11) (1975) 874–881.
[43] A. Sennaroglu, Photonics and Laser Engineering: Principles, Devices, and Applications, McGrew Hill, 2010.
[44] P. Laporta, N. Coluccelli, M. Tonelli, G. Galzerano, D. Parisi, F. Cornacchia, Tm-doped $LiLuF_4$ crystal for efficient laser action in the wavelength range from 182 to 206 μm, Opt. Lett. 32 (14) (2007) 2040.
[45] G. Galzerano, F. Cornacchia, D. Parisi, A. Toncelli, M. Tonelli, P. Laporta, Widely tunable 194-?mTm:BaY_2F_8 laser, Opt. Lett. 30 (8) (2005) 854.
[46] P. Ge, J. Liu, S. Jiang, Y. Xu, B. Man, Compact Q-switched 2 μm Tm:GdVO4 laser with MoS2 absorber, Photonics Res. 3 (5) (2015) 256–259.
[47] S. Shu, T. Yu, J. Hou, R. Liu, M. Huang, W. Chen, End-pumped all solid-state high repetition rate Tm, Ho:LuLF laser, Chinese Opt. Lett. 9 (2) (2011) 21401.
[48] B. Zhang, et al., Compact self-Q-switched Tm:YLF laser at 1.91 μm, Opt. Laser Technol. 100 (2018) 103–108.
[49] M. Segura, et al., Passive Q-switching of the diode pumped Tm^{3+}:$KLu(WO_4)_2$ laser near 2-μm with Cr^{2+}:ZnS saturable absorbers, Opt. Express 20 (4) (2012) 3394.
[50] F.X. Kärtner, L.R. Brovelli, D. Kopf, M. Kamp, I.G. Calasso, U. Keller, Control of solid state laser dynamics by semiconductor devices, Opt. Eng. 34 (7) (1995) 2024–2036.
[51] G.J. Sp?hler, et al., Experimentally confirmed design guidelines for passively Q-switched microchip lasers using semiconductor saturable absorbers, J. Opt. Soc. Amer. B 16 (3) (1999) 376.
[52] B.M. Walsh, N.P. Barnes, B. Di Bartolo, Branching. ratios, cross. sections, Branching ratios cross sections and radiative lifetimes of rare earth ions in solids: Application to Tm3+and Ho3+ions in LiYF4, J. Appl. Phys. 83 (5) (1998) 2772–2787.